

Expansion of Mitochondrial and Nuclear Heme Sensor Library

By: Pranusha Atuluru

School of Chemistry and Biochemistry
Georgia Institute of Technology
Principle Investigator: Amit Reddi
Graduate Student: Courtney Moore

Abstract

The long-term objective of the work in the lab is to determine the mechanisms by which cells sense and respond to the utilization of heme, an essential nutrient. Heme is an iron-containing compound of the porphyrin class that enables proteins to carry out an array of functions. Heme-dependent processes require that heme be dynamically mobilized to hemoproteins in almost every subcellular compartment. Although it is understood that the cytotoxicity and hydrophobicity of heme requires heme be tightly regulated by the cell, the method by which this is done is unknown [1]. The primary factor that limits the understanding of heme mobilization and trafficking is the lack of tools available to sense heme, more specifically labile heme. The Reddi lab is working to develop ratiometric fluorescent sensors to offer better insight into subcellular labile heme pools relevant for heme trafficking and signaling. HS1 (Heme Sensor 1) is mutated at either the His or Met in the heme-binding coordinating bundle of cytochrome to create sensors of different affinity. Ten new mutant sensors were created from the original HS1 and HS1-M7A, and it is seen that two sensors, H102C and H102C-M7H, are the most suitable sensors to be used in the mitochondria, nucleus and cytosol. With the use of these sensors, different pathways of heme trafficking and signaling can be studied in the cell.

Introduction

Heme is a critical life enabling metallonutrient required for virtually all life on Earth, serving as both a protein cofactor and signaling molecule. The total heme in the cell consists of exchange-inert and exchange-labile pools; inert heme is unavailable for new processes because it is tightly bound to heme enzymes. In contrast, labile heme is weakly bound and can readily be exchanged between proteins for trafficking and signaling [2]. Since labile heme is largely

involved in chemical processes, studying it is vital for understanding the mechanisms and dynamics of heme re-distribution in response to changes in cellular heme demand [1]. However, the properties of labile heme are poorly understood, largely in part due to the lack of tools to probe and measure it. The creation of these tools becomes more complicated since the subcellular distribution of LH is heterogeneous; the cytosol maintains LH at ~20–40 nM, but the mitochondria and nucleus maintain concentrations below 2.5 nM.

In the past, the Reddi Lab generated genetically encoded fluorescent heme sensors that can be targeted to the cytosol, mitochondria, and nucleus. Using this novel class of ratiometric fluorescent heme sensors in the model eukaryote, Baker's yeast, the Reddi lab has uncovered new heme trafficking factors and cellular processes that regulate the dynamics of heme mobilization [1]. However, in order to expand the utility of the sensors to other organisms, cell types, and subcellular compartments, a larger library of sensors with varying heme-binding affinities is required. The ideal sensor will be 50% bound to an analyte of interest so that both increases and decreases can be imaged. Currently, the previously published prototype heme sensors include HS1 and HS1-M7A. The first-generation heme sensor, HS1, was created with the heme-binding His/Met coordinating bundle in cytochrome b562 (Cyt b562) fused to a pair of fluorescent proteins, EGFP and Katushka 2 (mKATE2), which exhibit heme-sensitive and -insensitive fluorescence. HS1-M7A was generated by replacing the Met₇ ligand of Cyt b562 with Alanine. These sensors either have an extremely high heme affinity such that it is 100% saturated with heme or a more modest affinity that is ideal for cytosolic heme sensing (~30-50% bound) but not for nuclear or mitochondrial heme imaging (<10% bound), respectively. Herein we describe efforts to mutagenize HS1 in order to create a library of sensors that span the heme affinity space between HS1 and HS1-M7A. Successful completion of this goal will lead to better tools to probe heme homeostasis in human health and disease, including disorders that exhibit defects in heme

utilization and metabolism like Alzheimer's disease and a number of cancers.

Materials and Methods

The yeast strains used in the study were derived from BY4741 and the E.coli strains used were 10G cells from E.cloni. Yeast were cultured in yeast extract-peptone based medium supplemented with 2% glucose (YPD). The E.coli were cultured in Lysogeny broth (LB) with the appropriate antibiotic selection. The E.coli and yeast were transformed using HS1, which is the Heme Sensor Expression Plasmids that was generated by fusing mKATE2 and eGFP. mKATE2 and eGFP were used as the fluorescence tags where the eGFP de-fluoresces when heme is bound to it and mKATE2 fluoresces irrespective to heme. For all expression plasmids, heme variations were generated by Quick change mutagenesis [2]. HS1 was mutated at either the His or Met residues in the heme-binding coordinating bundle of cytochrome to create sensors of different affinity. For mitochondrial or nuclear targeting, heme sensors were fused to N-terminal Cox4 or C-terminal SV40 localization sequences.

For fluorescence experiments, the wild-type (WT) and heme-deficient *hem1Δ* yeast cells expressing the sensor plasmids were grown for 15-17 hours in SCE-LEU media. Optimal concentrations cells after growth were around 1 OD_{600nm}/mL and were taken on the Cary 60 spectrophotometer. In each experiment, HS1 and HS1-M7A sensors in WT and *hem1Δ* yeast are used as control. The cultured cells were further washed in water and resuspended in phosphate buffered saline (PBS) solution at concentrations between 8-10 OD_{600nm}/mL.

Fluorimetry measurements were collected on a Synergy Mx multi-modal plate reader using a black 96 well Greiner flat bottom plate. EGFP and mKATE fluorescence was recorded

using excitation wavelengths around 488nm and 588nm and emission wavelengths around 510nm and 620nm. Fluorescence of cells without heme sensors was also recorded as a blank and subtracted from eGFP and mKATE2 fluorescence values. With these values, the fractional saturation was calculated using the formula seen below.

$$\text{Fractional Saturation} = \frac{R_{\text{experimental}} - R_{\text{min}}}{R_{\text{max}} - R_{\text{min}}} * 100$$

R_{expt} is the EGFP:mKATE2 fluorescence ratio of the WT sensor. R_{min} is the EGFP:mKATE2 fluorescence ratio when 0% of the sensor is bound to heme, which in these experiments will be the experimental hem1Δ fluorescence ratio. R_{max} is the EGFP:mKATE2 fluorescence ratio when 100% of the sensor is bound to heme, which is the HS1 fluorescence ratio. Fractional saturation is a good analysis value in order to compare sensors to each other.

From the collection of ten mutant sensors, five with the most promising data were chosen for succinyl acetone (SA) and Aminolevulinic acid (ALA) titrations. WT HS1 and mutant sensor yeast were grown in different concentrations of succinyl acetone (see concentrations below). Hem1Δ HS1 and mutant sensor yeast were grown in different concentrations of Aminolevulinic acid (see concentrations below). After culturing, the same protocol as fluorimetry was followed. Two mutants of each sensor were done to improve validity of experiments.

Table 1: Concentrations of SA and ALA used in Titrations

[Succinyl Acetone] (in WT) Units: mM	[Aminolevulinic acid] (in hem1Δ) Units: μg/mL
0	0
25	5
50	15
100	30

150	50
200	100
500	200

Results

In the sensor, the fluorescence tag eGFP de-fluoresces when heme is bound to it while the mKATE2 fluoresces irrespective to heme; therefore, the higher the ratio of eGFP/mKATE, the less heme that is bound to the sensor. The fluorescence ratios were converted into fractional saturations using the equation shown in methods in order to display data.

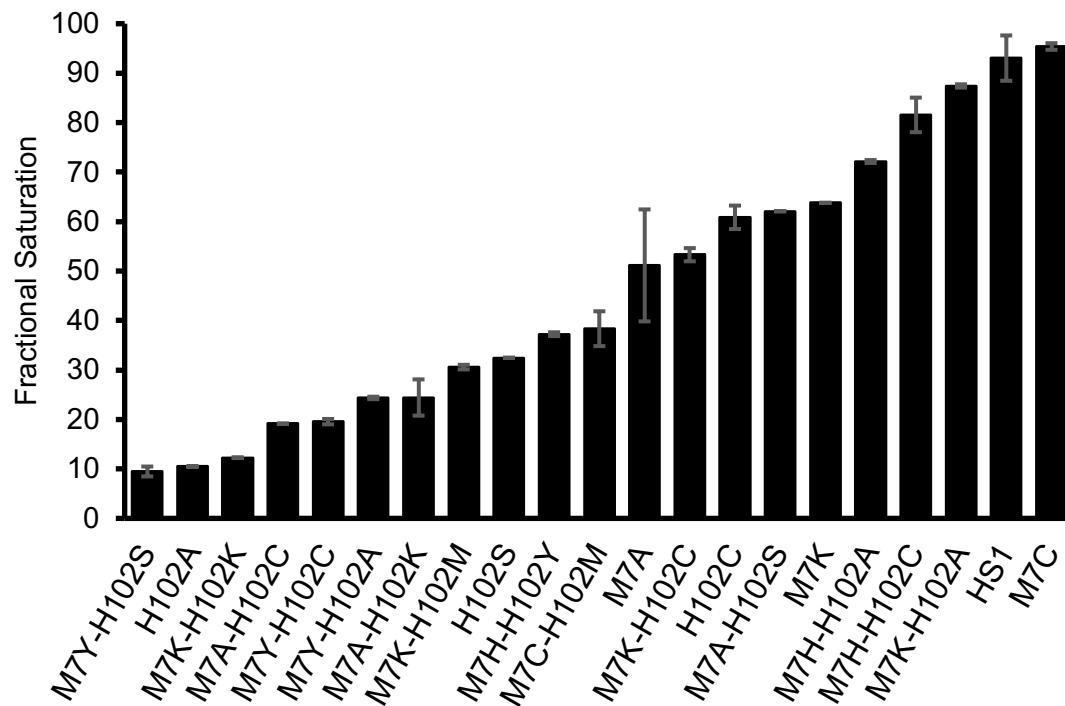
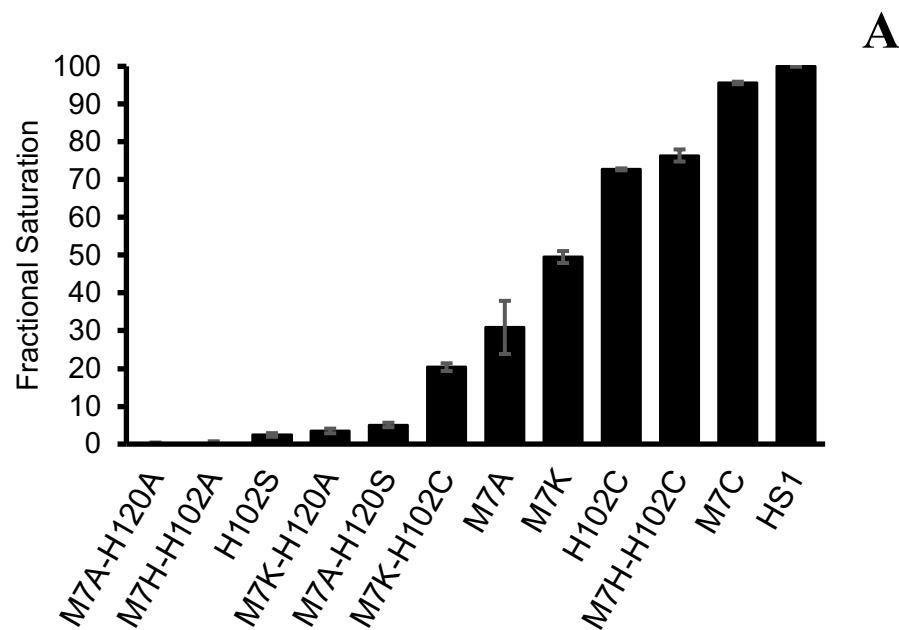


Figure 1: Fractional Saturations of Cytosolic Sensors. Heme saturation is the heme binding intensity of all sensors in regard to the 100% saturation of HS1.

The sensors created are targeted for the three organelles: nucleus, mitochondria, and cytosol. Previous data existed for the cytosolic sensors (Figure 1). In all three organelles, the HS1 WT and hem1Δ are used as control and have a fractional saturation of 100%. However, HS1-M7A had around a ~50% saturation in the cytosol and close to 0% in the nucleus/mitochondria. Therefore, to create sensors for the mitochondria and nucleus with reasonable saturation, all sensors in Figure 1 between HS1-M7A and HS1-M7C were created.

Although 10 sensors exist on the graph between HS1-M7A and HS1, 2 more heme sensors were created and tested for the nuclear library including H102A-M7A and H102S. The H102S sensor produced peculiar data in the nucleus and was discarded when moving sensor testing into the mitochondria. Therefore, only 11 sensors were tested in the mitochondria. The fractional saturations of the sensors in both organelles is displayed in Figure 2A/B.



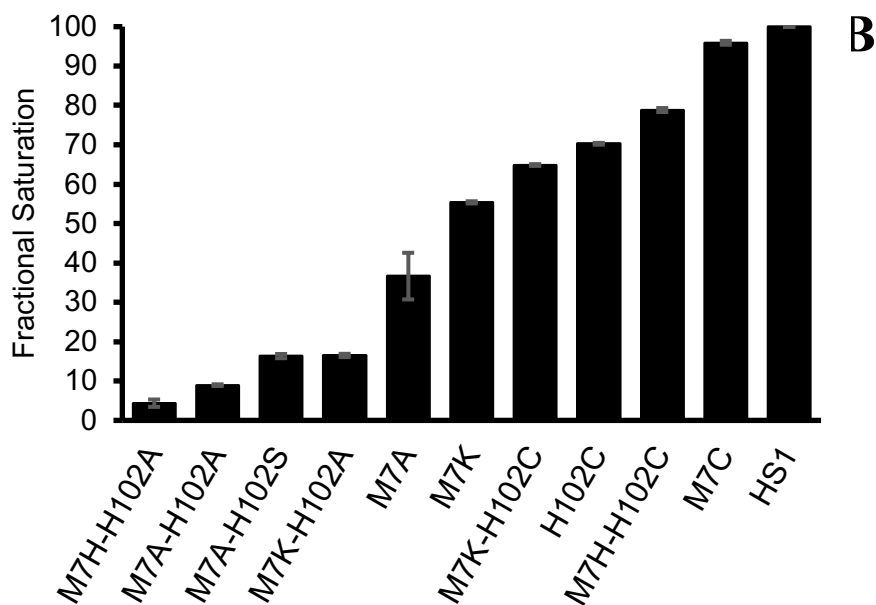


Figure 2: Nuclear and Mitochondrial Heme Sensors **A)** Nuclear sensor fractional saturations in regard to the 100% saturation of nuclear-HS1. **B)** Mitochondrial sensor fractional saturations in regard to the 100% saturation of mitochondrial-HS1.

Table 2: Numerical Fractional Saturations of sensors in the Cytosol, Nucleus and Mitochondria

Sensors	Cytosol	Nucleus	Mitochondria
M7A	51.14	30.89	36.64
M7K-H102C	53.30	20.37	64.86
H102C	60.87	72.73	70.25
M7A-H102S	62.09	5.07	16.33
M7K	63.79	49.52	55.37
M7H-H102A	72.14	0.00	4.37
M7H-H102C	81.56	76.40	78.82
M7K-H102A	87.42	3.48	16.50
M7C	95.39	95.60	95.90
HS1	100.00	100.00	100.00
M7A-H102A		0.00	8.95
H102S		2.42	

Table 2 displays the numerical fractional saturations of each sensor in each organelle.

From the table, five sensors, excluding HS1, with a fractional saturation between 50-100% are chosen to for SA and ALA titrations. The five selected sensors and the HS1 sensor are displayed

in Figure 3. Refer to the methods for more details on the titration procedures. Titrations were done to test whether sensors are able to detect variations in heme concentrations in different cells. Succinyl Acetone is added to WT cells to suppress heme synthesis while Aminolaevulinic acid is added to hem1Δ cells to promote heme synthesis. Titrations were done on two different clones and were averaged for improved accuracy.

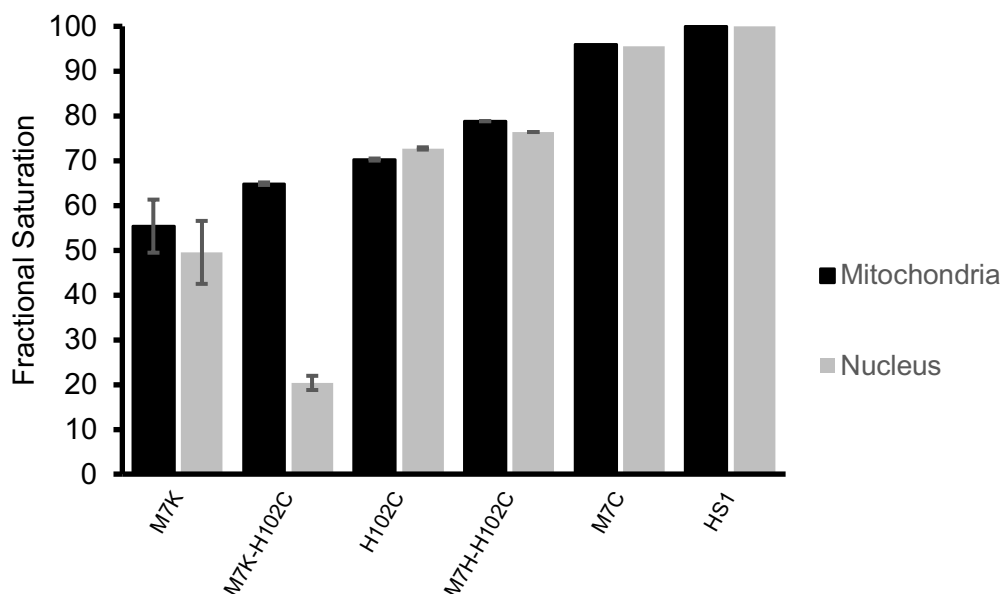


Figure 3: Nuclear and Mitochondrial fractional saturations for the six sensors chosen for SA/ALA Titrations.

Figures 4-9 show the SA/ALA titration fractional saturations of the five selected sensors in each cell compartment. Since ALA promotes heme synthesis, the fractional saturations of the hem1Δ cells should increase as the concentration of ALA increases. On the other hand, since SA inhibits heme synthesis, the fractional saturations of the WT cells should decrease as the concentration of the SA increase.

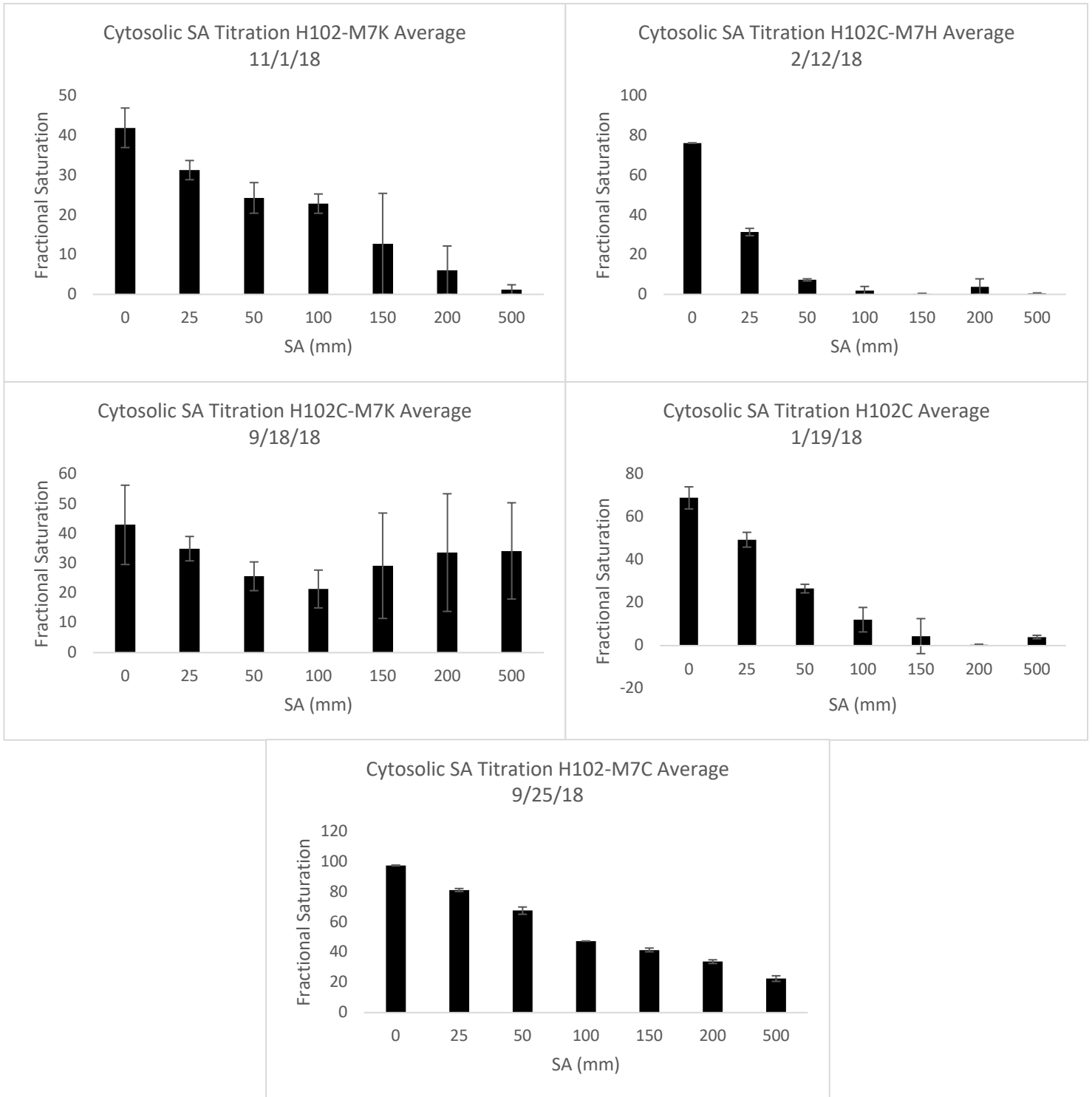


Figure 4: Fraction Saturations for SA titrations of the five cytosolic sensors. These are averages of two different mutants.

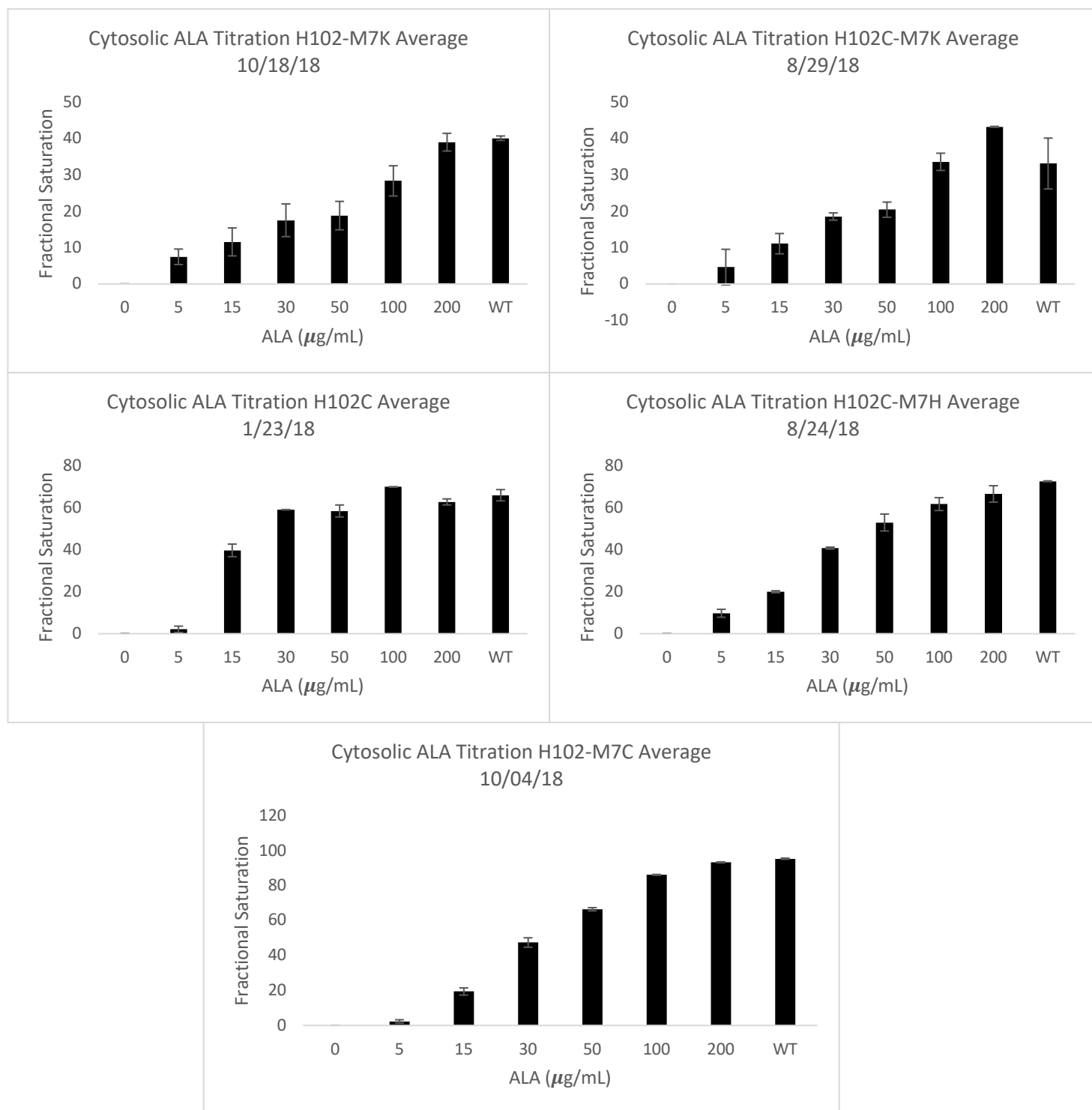


Figure 5: Fraction Saturations for ALA titrations of the five cytosolic sensors. These are averages of two different mutants.

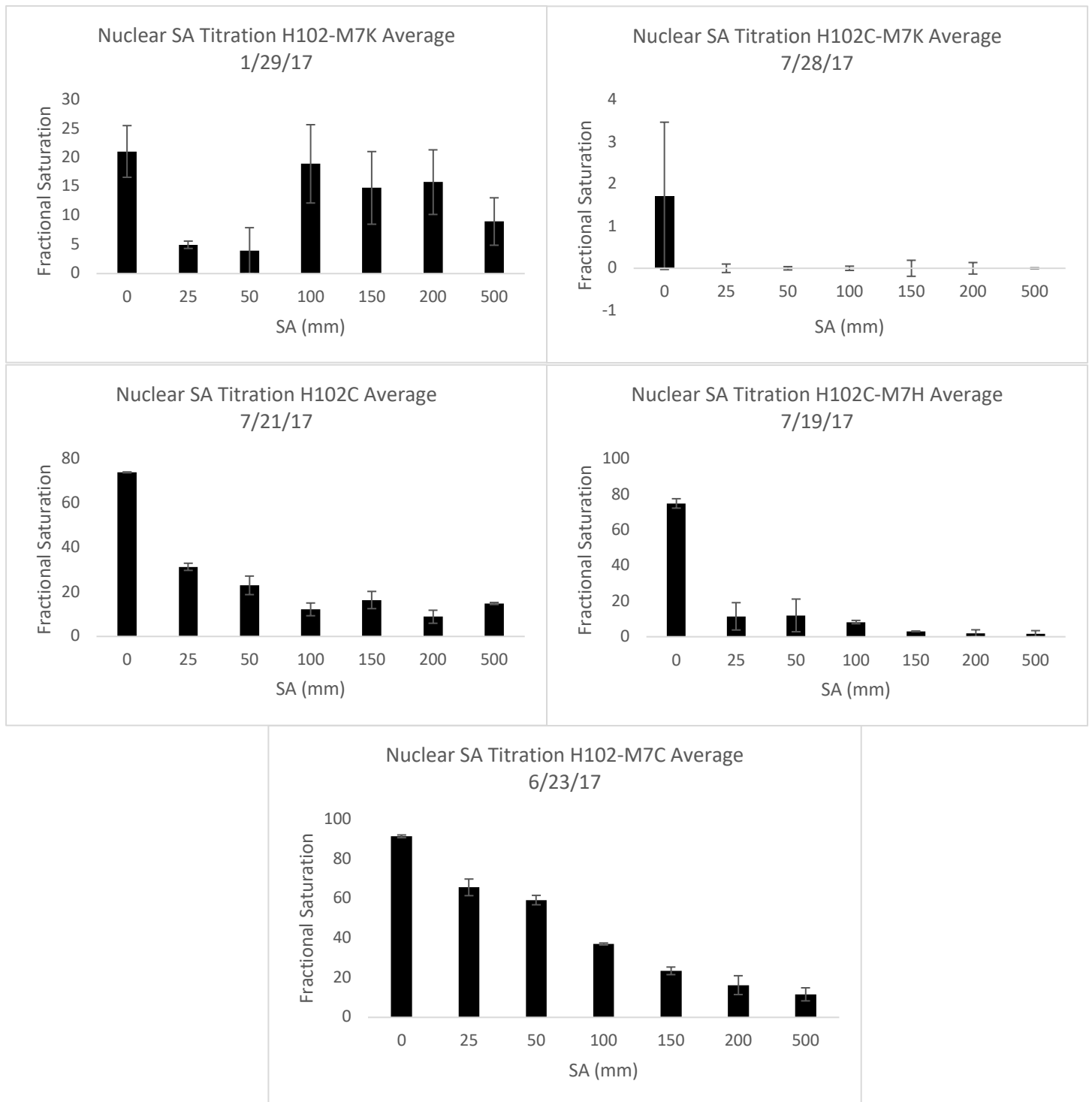


Figure 6: Fraction Saturations for SA titrations of the five nuclear sensors. These are averages of two different mutants.

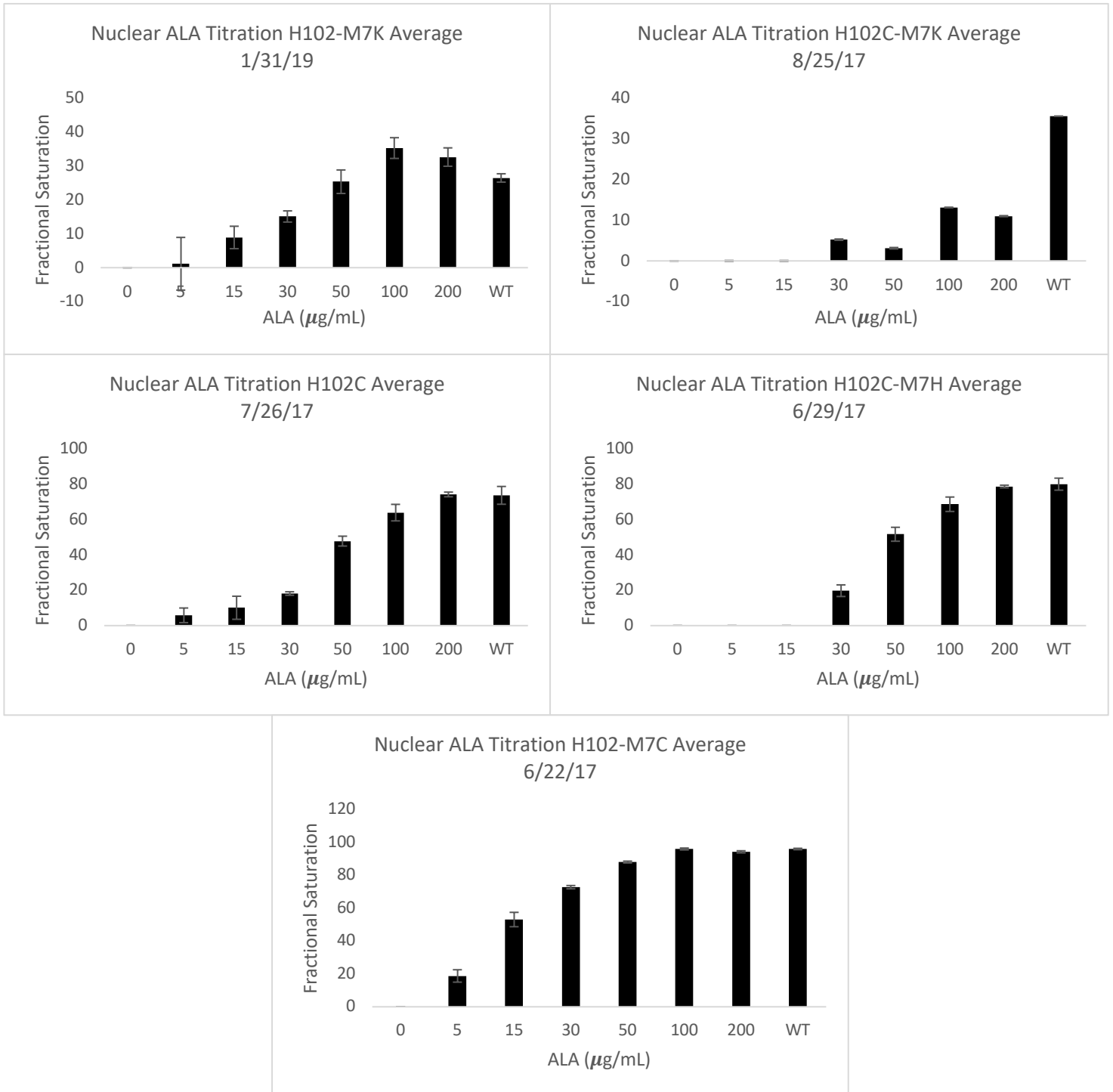


Figure 7: Fraction Saturations for ALA titrations of the five nuclear sensors. These are averages of two different mutants.

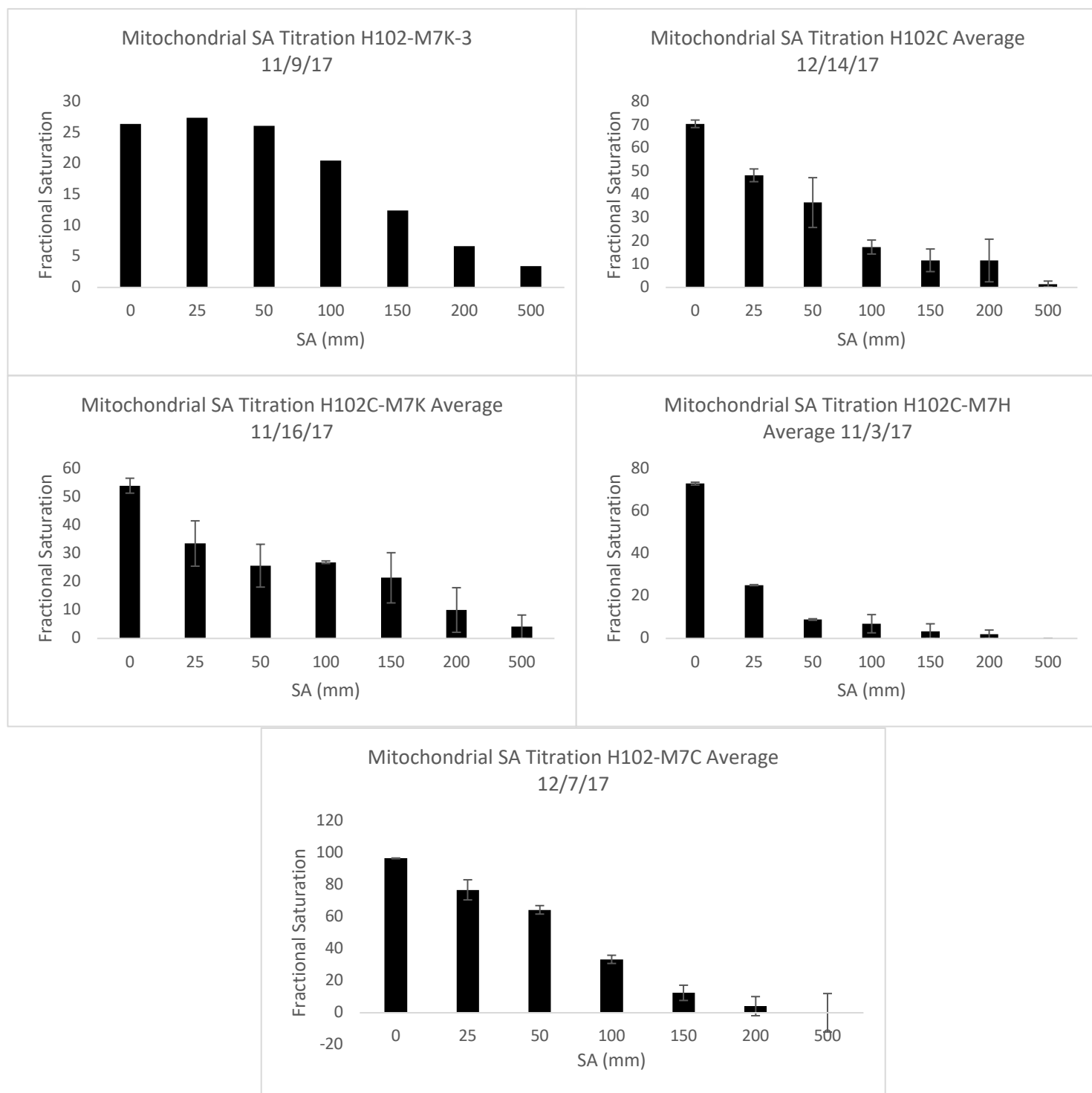


Figure 8: Fraction Saturations for SA titrations of the five mitochondrial sensors. These are averages of two different mutants.

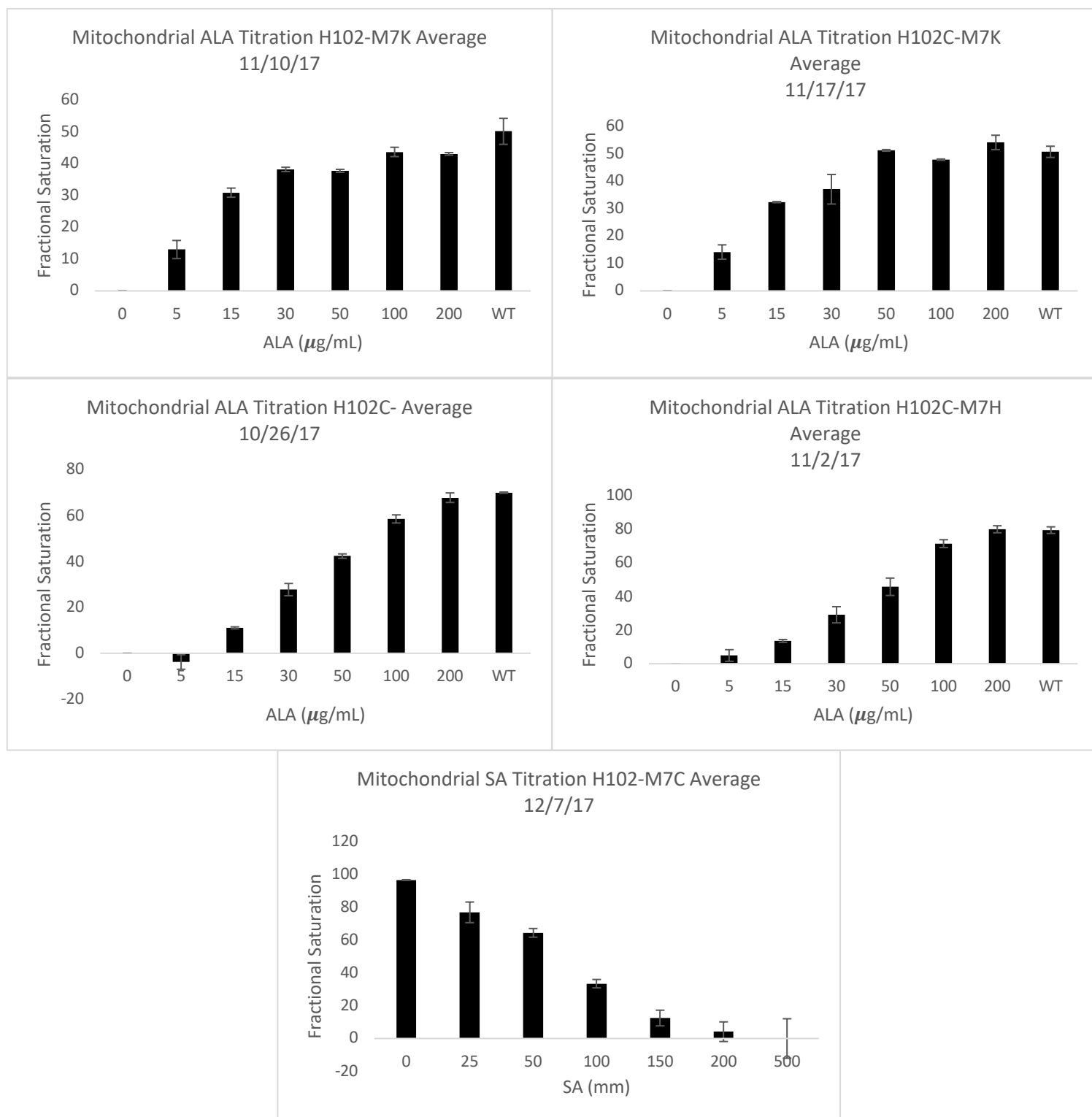


Figure 9: Fraction Saturations for ALA titrations of the five mitochondrial sensors. These are averages of two different mutants.

Discussion

Over the years, twelve nuclear sensors and eleven mitochondrial sensors were created to expand the heme library. The most useful and applicable sensors should have a fractional saturation around 50%. Initially it was thought that HS1-M7A had around a 0% fractional saturation in the mitochondria and nucleus. From the new fluorescence experiments, the actual value was found to be around 30.89% with a standard deviation of 7.03% in the nucleus and 36.64% with a standard deviation of 5.90% in the mitochondria.

Some of the heme sensors did not show the expected results in the nucleus and mitochondria. For example, H102C had a fractional saturation of ~61% in the cytosol. When tested in the mitochondrial and nucleus, the fractional saturation increased to ~70-72%. Although the mitochondria and nucleus have significantly lower levels of labile heme, the sensor was more saturated. Further, H102C-M7K had fractional saturations of around ~53% and ~65% in the cytosol and mitochondrial but had a fractional saturation of around ~20% in the mitochondria. Other types of sensors like H102C-M7H also existed where the sensor has similar fractional saturations in all three compartments.

The different patterns in the various sensors could exist for a multitude of reasons. One of them could be due to differences in oxidation-state selectivity, where some of the sensors could specifically be measuring ferrous (+2) heme or ferric (+3) heme over the other. However, it is not fully understood whether each compartment consists of more ferric or ferrous heme to draw conclusions about the sensors. More experiments need to be conducted to understand the different patterns seen in each sensor. A method of doing this is to purify and characterize the sensor proteins outside of the cellular environment. This would allow to directly select whether ferrous or ferric heme existed in the solution to test the sensors.

Since the most applicable sensors should have a fractional saturation around 50%, five specific sensors were chosen for titrations and further testing: HS1-M7K, H102C, H102-M7H, HS1-M7C, and H102C-M7K. Most of the sensors functioned as expected where the fractional saturation decreased as the amount of SA was increased and it increased as the amount of ALA was increased. Cytosolic H102C-M7K and nuclear HS1-M7K did not have a similar pattern, but had extremely high standard deviations; therefore, more mutants should be run to acquire a more accurate response. Some of the sensors like nuclear H102C-M7K had a low fractional saturation of 3% from the titrations but had a 20-30% fractional saturation when tested in fluorescence experiments. In order to test whether this is from experimental error or valid results, more trials with mutants should be run and experiments should be done with the purified sensor outside of the cell.

Moving forward, more characterization experiments need to be conducted with the sensors to understand how they behave in different environments. Nickel column chromatography and HPLC experiments can be done to purify the sensors and heme titrations can be done with these sensors outside of the cell. This is to ensure that other factors didn't affect the fractional saturation of the sensors and confirm that heme affinity matches the saturation. This also provides experimentation to deduce the heme dissociation constants for each sensor (K_D), which gives a numerical value to the heme affinities of each sensor. The K_D of the heme sensor should be similar to the concentration of the labile heme in order to ensure that the sensor is around 50% bound with heme [2].

Other challenges could also be encountered when further developing sensors of the correct affinity for each compartment. One of these is to ensure that sensor expression does not affect heme homeostasis in the cell [2]. It was previously predicted that lower-affinity sensors

are less disruptive to the measurement of labile heme; however, the lower-affinity sensors are less saturated and cannot deduce changes in heme at lower concentrations as easily. Therefore, individual experiments with the sensors need to be done to determine the effect of sensor expression on the labile heme concentration.

Conclusion

It is imperative to understand heme cell biology and heme trafficking due to heme's role in many physiological diseases/illnesses such as Alzheimer's and cancer. However, the largest barrier to properly understand heme is the lack of tools available to properly sense labile heme. Therefore, in recent years there has been an increase in the creation of innovative methods to better detect and understand heme within individual cells. One of these methods is the creation of genetically encoded heme sensors with saturations around 50% to properly detect changes in heme concentration in cells. Creating a proper library of cytosolic, mitochondrial, and nuclear sensors will greatly expand the tools available to better understand heme mechanisms and signaling in the body. Although there is a lot more work to be done with understanding heme sensor binding affinities, oxidation-state selectivity, and sensors' effect on heme homeostasis, the heme sensors have the ability to revolutionize our understanding of intracellular heme sensing and distribution, which could allow for better understanding of disease physiologies.

References

- [1] Reddi, A. R., & Hamza, I. (2016). Heme Mobilization in Animals: A Metallolipid's Journey. *Accounts of Chemical Research*, 49(6), 1104-1110.
- [2] Hanna, D. A., Harvey, R. M., Martinez-Guzman, O., Yuan, X., Chandrasekharan, B., Raju, G., . . . Reddi, A. R. (2016). Heme dynamics and trafficking factors revealed by genetically encoded fluorescent heme sensors. *Proceedings of the National Academy of Sciences*, 113(27), 7539-7544.
- [3] van Manen HJ, Uzunbajakava N, van Bruggen R, Roos D, Otto C. Resonance Raman Imaging of the NADPH Oxidase Subunit Cytochrome B558 in Single Neutrophilic Granulocytes. *J. Am. Chem. Soc.* 2003; 125:12112–12113.
- [4] Lu S, Min W, Chong S, Holtom GR, Xie XS. Label-Free Imaging of Heme Proteins with Two-Photon Excited Photothermal Lens Microscopy. *Appl. Phys. Lett.* 2010; 96:113701
- [5] Hanna DA, Martinez-Guzman O, Reddi AR. Heme Gazing: Illuminating Eukaryotic Heme Trafficking, Dynamics, and Signaling with Fluorescent Heme Sensors. *Biochemistry*. 2017;56(13):1815-1823.
- [6] Arpino, J. A., Czapinska, H., Piasecka, A., Edwards, W. R., Barker, P., Gajda, M. J., . . . Jones, D. D. (2012). Structural Basis for Efficient Chromophore Communication and Energy Transfer in a Constructed Dimer Protein Scaffold. *Journal of the American Chemical Society*, 134(33), 13632-13640.
- [7] Hanna, D. A., Harvey, R. M., Martinez-Guzman, O., Yuan, X., Chandrasekharan, B., Raju, G., . . . Reddi, A. R. (2016). Heme dynamics and trafficking factors revealed by genetically encoded fluorescent heme sensors. *Proceedings of the National Academy of Sciences*, 113(27), 7539-7544.